Article

Metal and Ligand K-Edge XAS of Organotitanium Complexes: Metal 4p and 3d Contributions to Pre-edge Intensity and Their Contributions to Bonding

Serena DeBeer George, Patrick Brant, and Edward I. Solomon

J. Am. Chem. Soc., **2005**, 127 (2), 667-674• DOI: 10.1021/ja044827v • Publication Date (Web): 21 December 2004

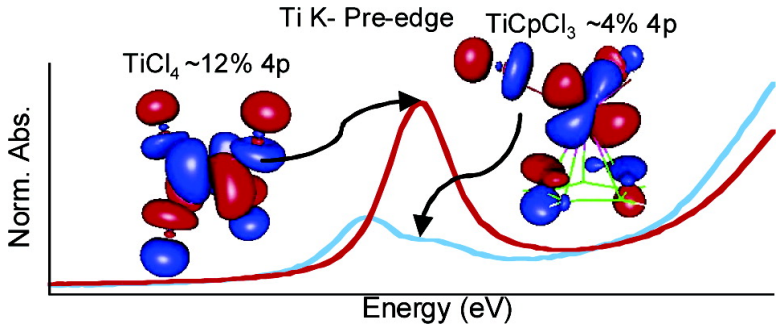

More About This Article

Additional resources and features associated with this article are available within the HTML version:

- Supporting Information
- Links to the 8 articles that cite this article, as of the time of this article download
- Access to high resolution figures
- Links to articles and content related to this article
- Copyright permission to reproduce figures and/or text from this article

View the Full Text HTML

J|A|C|S
ARTICLES
Published on Web 12/21/2004

Metal and Ligand K-Edge XAS of Organotitanium Complexes: Metal 4p and 3d Contributions to Pre-edge Intensity and Their Contributions to Bonding

Serena DeBeer George,*,† Patrick Brant,‡ and Edward I. Solomon*,§

Contribution from the Stanford Synchrotron Radiation Laboratory, SLAC, Stanford University, Stanford, California 94309, Baytown Polymer Center, ExxonMobil Chemical Company, Baytown, Texas 77522, and Department of Chemistry, Stanford University, Stanford, California 94305

Received August 26, 2004; E-mail: Edward.Solomon@Stanford.edu; serena@slac.stanford.edu

Abstract: Titanium cyclopentadienyl (Cp) complexes play important roles as homogeneous polymerization catalysts and have recently received attention as potential anticancer agents. To systematically probe the contribution of the Cp to bonding in organotitanium complexes, Ti K-edge XAS has been applied to $TiCl_4$ and then to the mono- and bis-Cp complexes, $TiCpCl_3$ and $TiCp_2Cl_2$. Ti K-edge XAS is used as a direct probe of metal 3d−4p mixing and provides insight into the contribution of the Cp to bonding. These data are complimented by Cl K-edge XAS data, which provide a direct probe of the effect of the Cp on the bonding to the spectator chloride ligand. The experimental results are correlated to DFT calculations. A model for metal 3d−4p mixing is proposed, which is based on covalent interactions with the ligands and demonstrates that metal K-pre-edge intensities may be used as a measure of ligand−metal covalency in molecular Ti(IV) systems in noncentrosymmetric environments.

I. Introduction

Since the mid-1950s, there has been considerable interest in understanding the chemistry of organotitanium complexes.[1−7] Much of the research has focused on the ability of mono- and bis-cyclopentadienyl (Cp) complexes to act as homogeneous polymerization catalysts.[1−3,5] The reactivity of titanium complexes is often correlated to the site symmetry and the oxidation state of the catalyst,[2,8−10] and hence insight into the electronic structure could assist in understanding reactivity. In addition to their role as polymerization catalysts, organotitanium complexes have recently received attention as potential anticancer agents.[11−13] Titanium bis-cyclopentadienyl dichloride is currently in phase II clinical trials as a treatment for leukemia, melanoma, and colon and lung carcinomas.[14,15] The mechanism is unknown, but a bis-cylopentadienyl-titanium-DNA complex has been implicated in the antitumor activity.[11] Hence, a detailed understanding of the contribution of the cyclopentadienyl ligand to bonding in titanium complexes and the potential labilization of chloride has broad interest in both organometallic and bioinorganic chemistry.

X-ray absorption spectroscopy (XAS) is a direct method for experimentally probing the electronic structure of organotitanium complexes. Metal K-edge XAS can provide information about the oxidation state of a metal site and in certain cases may be used to determine the coordination number, site-symmetry, and spin-state.[16−18] A detailed Fe K-edge study on a series of model complexes has shown that the energies and intensities of the 1s to 3d pre-edge features vary systematically with changes in electronic structure and can be evaluated by a multiplet analysis.[16] A 1s to 3d transition is formally electric dipole forbidden but can gain intensity through either a quadrupole mechanism or through metal 4p mixing with the 3d orbitals, giving the transition electric dipole allowed character. Since a quadrupole transition is ∼2 orders of magnitude weaker than a dipole transition, 4p mixing while small can have a significant contribution to the intensity of the pre-edge feature. By group theory, 3d−4p mixing may only occur in noncentrosymmetric

† Stanford Synchrotron Radiation Laboratory, Stanford University.
‡ ExxonMobil Chemical Co.
§ Department of Chemistry, Stanford University.

(1) Alt, H. G.; Köppl, A. *Chem. Rev.* **2000**, *100*, 1205.
(2) Coates, G. W. *Chem. Rev.* **2000**, *100*, 1223.
(3) Hlatky, G. G. *Coord. Chem. Rev.* **1999**, *181*, 243.
(4) Green, J. C. *Chem. Soc. Rev.* **1998**, *27*, 263.
(5) Britzinger, H. H.; Fischer, D.; Mülhaupt, R.; Rieger, B.; Waymouth, R. M. *Angew. Chem.* **1995**, *34*, 1143.
(6) Natta, G.; Pino, P.; Mazzanti, G.; Giannini, U. *J. Am. Chem. Soc.* **1957**, *79*, 2975.
(7) Ziegler, K.; Holzkamp, E.; Breil, H.; Martin, H. *Angew. Chem.* **1955**, *67*, 541.
(8) Grassi, A.; Saccheo, S.; Zambelli, A.; Laschi, F. *Macromolecules* **1998**, *31*, 5588.
(9) Williams, E. F.; Murray, M. C.; Baird, M. C. *Macromolecules* **2000**, *33*, 261.
(10) Mahanthappa, M. K.; Waymouth, R. M. *J. Am. Chem. Soc.* **2001**, *123*, 12093.
(11) Harding, M. M.; Mokdsi, G. *Curr. Med. Chem.* **2000**, *7*, 1289.
(12) Guo, M.; Guo, Z.; Sadler, P. J. *J. Biol. Inorg. Chem.* **2001**, *6*, 698.
(13) Guo, M.; Sadler, P. J. *Dalton* **2000**, *1*, 7.
(14) Köpf-Maier, P. *Anticancer Res.* **1999**, *19*, 493.
(15) Kroger, N.; Kleeberg, U. R.; Mross, K.; Edler, L.; Sass, G.; Hossfeld, D. K. *Onokologie* **2000**, *23*, 60.
(16) Westre, T. E.; Kennepohl, P.; DeWitt, J. G.; Hedman, B.; Hodgson, K. O.; Solomon, E. I. *J. Am. Chem. Soc.* **1997**, *119*, 6297.
(17) Kau, L. S.; Spira-Solomon, D. J.; Penner-Hahn, J. E.; Hodgson, K. O.; Solomon, E. I. *J. Am. Chem. Soc.* **1987**, *109*, 6433.
(18) DuBois, J. L.; Mukherjee, P.; Solomon, E. I.; Stack, T. D. P.; Hodgson, K. O. *J. Am. Chem. Soc.* **2000**, *122*, 5775.

environments, and hence the pre-edge features of centrosymmetric complexes are very weak. Systematic metal K-edge studies have also been applied to other first-row transition metals, including titanium.[19−21] However, previous Ti K-edge studies have focused primarily on Ti-oxides and relatively little is understood about the contribution of organometallic bonding to the Ti K-edge structure.[22,23] Hence, these studies will also be important in defining the nature of Ti−Cp bonding.

Ligand K-edge XAS can provide complimentary information to the metal K-edge XAS data. Previous studies have shown that the Cl K-pre-edge feature can be used as a direct probe of Cl 3p character in the unoccupied d orbitals.[24,25] Previous studies have shown that ligand K-edge XAS is a useful method for examining spectator ligand effects in iron−sulfur clusters.[26] Here, it is used to probe the covalency of Ti−Cl bonds in organotitanium complexes.

To systematically probe the contribution of the Cp to bonding in organotitanium complexes, Ti K-edge XAS is first applied to $TiCl_4$ as a calibrant and then to the mono- and bis-Cp complexes, $TiCpCl_3$ and $TiCp_2Cl_2$, to obtain experimental insight into the Ti−Cp bond. These data are interpreted through a configuration interaction model in terms of the origin of metal 3d−4p mixing. Previous studies have addressed metal 3d−4p mixing in terms of symmetry arguments and ligand field effects and have not considered covalent interactions with the ligands.[16,27] These data are complimented by Cl K-edge XAS data which provide a direct probe of the effect of the Cp on the bonding to the spectator chloride ligand. The experimental results are correlated to DFT calculations. The theoretical 4p mixing into the 3d orbitals is correlated to experimental energy splittings and intensities and allows for an estimate of the quadrupole contribution to the pre-edge. The strong correlation between experiment and theory is of particular importance in understanding the contributions of Cp to bonding and its effect on pre-edge intensities.

II. Experimental Section

A. Sample Preparation. $TiCl_4$, $TiCpCl_3$, and $TiCp_2Cl_2$ were purchased from Strem Chemicals and were used without further purification. All samples were prepared in an inert atmosphere glovebox. $TiCl_4$ was measured as a dilute solution (10 mM for Ti K-edge measurement; 2−3 mM for Cl K-edge measurements) in dry, degassed toluene. $TiCpCl_3$ and $TiCp_2Cl_2$ were measured as solids. For Ti K-edge measurement, solids were diluted with graphite (which had been stirred in hot HCl, washed with ethanol, and dried in vacuo) and pressed into 0.5-mm-thick Al spacers sealed with 38-μm Kapton windows. For Cl K-edge measurements, solid samples were ground into a fine powder and dispersed as thinly as possible on Mylar tape.

B. X-ray Absorption Spectroscopy and Measurements and Data Analysis. All data were measured at the Stanford Synchrotron Radiation Laboratory under ring conditions of 3.0 GeV and 60−100 mA. Data were measured using the 54-pole wiggler beam line 6-2 in high magnetic field mode of 10 kG with a Ni-coated harmonic rejection mirror and a fully tuned (5366 eV for the Ti K-edge and 3150 eV for the Cl K-edge) Si(111) double crystal monochromator. Details of the optimization of this setup for low-energy studies have been described previously.[28]

(i) Ti K-edges. All Ti K-edge measurements were made at room temperature. Solution samples were measured as fluorescent spectra, using a Lytle detector.[29,30] Solids were measured as transmission spectra. To check for reproducibility, two to three scans were measured for all samples. The energy was calibrated from Ti foil spectra run at intervals between sample scans. The first inflection point of the Ti foil was fixed at 4966.0 eV. A step size of 0.11 eV was used over the edge region. Data were averaged, and a smooth background was removed from all spectra by fitting a polynomial to the pre-edge region and subtracting this polynomial from the entire spectrum. Normalization of the data was accomplished by fitting a flattened polynomial or straight line to the post-edge region and normalizing the edge jump to 1.0 at 5000 eV. Fits to the edges were performed using the program EDG_FIT.[31] Second-derivative spectra were used as guides to determine the number and position of peaks. pre-edge and rising edge features were modeled by pseudo-Voigt line shapes. For the pre-edge feature, a fixed 1:1 ratio of Lorentzian to Gaussian contributions was used. Fits were performed over several energy ranges. The reported intensity values and standard deviations are based on the average of all good fits. Normalization procedures can introduce ∼3% error in pre-edge peak intensities, in addition to the error resulting from the fitting procedure.

(ii) Cl K-Edges. All Cl K-edge measurements were made at room temperature. All data were measured as both fluorescence and electron yield spectra to monitor for possible self-absorption effects. To check for reproducibility, two to three scans were measured for each of the solid samples. The energy was calibrated from D_{2d}-$[Cs_2CuCl_4]$ spectra run at intervals between sample scans. The maximum of the first pre-edge feature in the spectrum was fixed at 2820.20 eV. A step size of 0.07 eV was used over the edge region. Data were averaged, and a smooth background was removed from all spectra by fitting a polynomial to the pre-edge region and subtracting this polynomial from the entire spectrum. Normalization of the data was accomplished by fitting a flattened polynomial or straight line to the post-edge region and normalizing the edge jump to 1.0 at 2840 eV. Fits to the Cl K-edge data were performed in the same manner as described for the Ti K-edge data above.

C. Electronic Structure Calculations. Density functional calculations (BP86) were carried out using ADF2000 on a Silicon Graphics Origin 2000 multiprocessor computer.[32,33] A triple-ζ Slater-type orbital basis set (ADF basis set IV) with a single polarization function at the local density approximation of Vosko et al.[34] and the nonlocal gradient corrections of Becke[35] and Perdew[36] were employed. The crystal structures of $TiCl_4$,[37] $TiCpCl_3$,[38] and $TiCp_2Cl_2$[39] were used as initial input models for the geometry optimizations (the coordinate system is

(19) Fraile, J. M.; García, J.; Mayoral, J. A.; Proietti, M. G.; Sánchez, M. C. *J. Phys. Chem.* **1996**, *100*, 19484.
(20) Farges, F.; Brown, G. E., Jr.; Rehr, J. J. *Phys. Rev. B* **1997**, *56*, 1809.
(21) Matsuo, S.; Sakaguchi, N.; Obuchi, E.; Nakano, K.; Perera, R. C. C.; Watanabe, T.; Matsuo, T.; Wakita, H. *Anal. Sci.* **2001**, *17*, 149.
(22) Wasserman, E. P.; Westwood, A. D.; Zhengtian, Y.; Oskam, J. H.; Duenas, S. L. *J. Mol. Catal. A* **2001**, *172*, 67.
(23) Thomas, J. M.; Sankar, G. *Acc. Chem. Res.* **2001**, *34*, 571.
(24) Solomon, E. I.; Hedman, B.; Hodgson, K. O.; Dey, A.; Szilagyi, R. K. *Coord. Chem. Rev.* In press.
(25) Glaser, T.; Hedman, B.; Hodgson, K. O.; Solomon, E. I. *Acc. Chem. Res.* **2000**, *33*, 859.
(26) Glaser, T.; Rose, K.; Shadle, S. E.; Hedman, B.; Hodgson, K. O.; Solomon, E. I. *J. Am. Chem. Soc.* **2001**, *123*, 442.
(27) Arrio, M.-A.; Rossano, S.; Brouder, C.; Galoisy, L.; Calas, G. *Europhys. Lett.* **2000**, *51*, 454.
(28) Hedman, B.; Frank, P.; Gheller, S. F.; Roe, A. L.; Newton, W. E.; Hodgson, K. O. *J. Am. Chem. Soc.* **1988**, *110*, 3798.
(29) Lytle, F. W.; Greegor, R. B.; Sandstrom, D. R.; Marques, E. C.; Wong, J.; Spiro, C. L.; Huffman, G. P.; Huggins, F. E. *Nucl. Instrum. Methods* **1984**, *226*, 542.
(30) Stern, E. A.; Heald, S. M. *Rev. Sci. Instrum.* **1979**, *50*, 1579.
(31) George, G. N. Stanford Synchrotron Radiation Laboratory, Stanford Linear Accelerator Center, Stanford University, Stanford, CA 94309.
(32) te Velde, G.; Bickelhaupt, F. M.; Baerends, E. J.; Guerra, C. F.; van Ginsberg, S. J. A.; Snijders, J. G.; Ziegler, T. *J. Comput. Chem.* **2001**, *22*, 931.
(33) Baerends, E. J.; Ellis, D. E.; Ros, P. *Chem. Phys.* **1973**, *2*, 41.
(34) Vosko, S. H.; Wilk, L.; Nusair, M. *Can. J. Phys.* **1980**, *58*, 1200.
(35) Becke, A. D. *Phys. Rev. A* **1988**, *38*, 3098.
(36) Perdew, J. P. *Phys. Rev. B* **1986**, *33*, 8822.
(37) Troyanov, S. I.; Snigireva, E. M. *Russian J. Inorg. Chem.* **2000**, *45*, 580.
(38) Engelhardt, L. M.; Papasergio, R. I.; Raston, C. L.; White, A. H. *Organometallics* **1984**, *3*, 18.
(39) Tkachev, V. V.; Atovmyan, L. O. *Zh. Strukt. Khim.* **1972**, *13*, 287.

Scheme 1

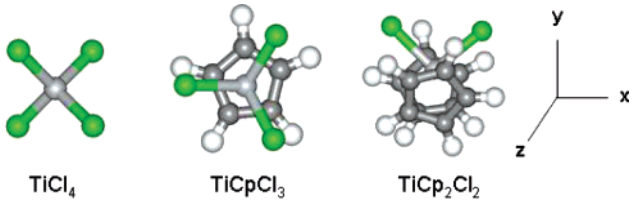

given in Scheme 1). Geometry optimization of $TiCl_4$ was performed in T_d symmetry. No symmetry was imposed for $TiCpCl_3$ or $TiCp_2Cl_2$ optimizations. The optimized coordinates show only very small deviations (changes of less than 0.02 Å in bond length and 0.5° in angle) relative to the crystal structures and are provided in the Supporting Information.

III. Results

Figure 1 shows a comparison of the normalized Ti K-edge spectra for $TiCl_4$, $TiCpCl_3$, and $TiCp_2Cl_2$. All three spectra are dominated by an intense 1s to 4p "edge" transition at ~4980 eV. Weaker, pre-edge transitions appear at ~4969 eV. The pre-edge transitions are 1s to 3d, which are formally electric dipole forbidden, but will have a small quadrupole contribution and may gain intensity through mixing of the metal 4p orbitals with the five unoccupied 3d orbitals. The relative intensities and energy distributions for all three complexes are given in Table 1. The pre-edge feature is clearly most intense for $TiCl_4$, which has a single intense feature at 4969.2 eV, with an integrated intensity of 58.4 units. For $TiCpCl_3$, the intensity of the pre-edge feature decreases by a factor of ~2 and the intensity distribution changes, with two peaks clearly visible in the pre-edge region. For $TiCp_2Cl_2$, the pre-edge intensity is further decreased by approximately a factor of 6 lower than for $TiCl_4$.

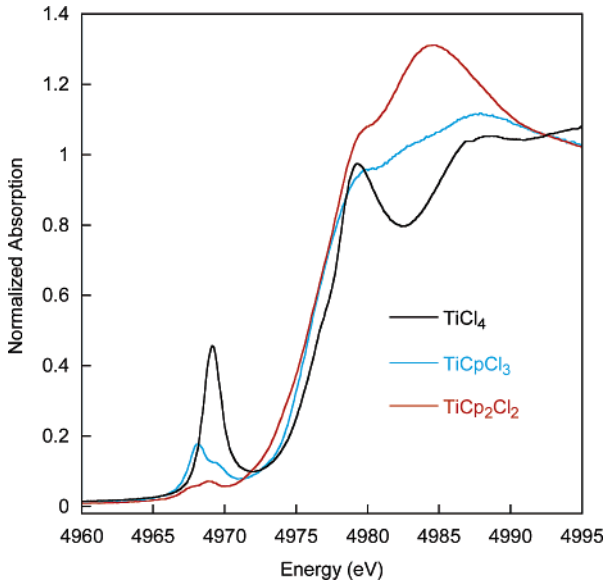

Figure 1. Comparison of the normalized Ti K-edge spectra for $TiCl_4$, $TiCpCl_3$, and $TiCp_2Cl_2$.

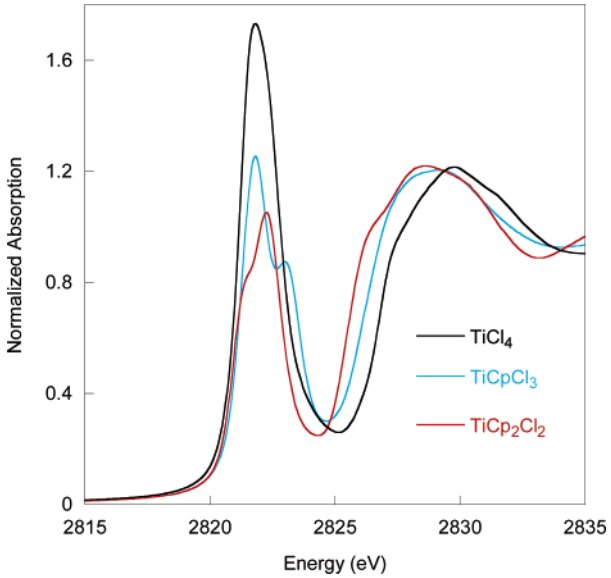

Figure 2. Comparison of the normalized Cl K-edge spectra for $TiCl_4$, $TiCpCl_3$, and $TiCp_2Cl_2$.

A comparison of the normalized Cl K-edge spectra for $TiCl_4$, $TiCpCl_3$, and $TiCp_2Cl_2$ is given in Figure 2. The pre-edges clearly show differences in intensity (per Ti−Cl bond), with $TiCl_4$ being the most intense, followed by $TiCpCl_3$, and then $TiCp_2Cl_2$ (Table 2). The decrease in pre-edge intensity reflects a decrease in the covalency of the Ti−Cl bond upon replacement of a Cl ligand by a Cp. These differences are described quantitatively in the analysis section. In all cases, two peaks were required to fit the pre-edge data. The energies and intensities of these features are given in Table 2. The rising edge inflection point shifts to lower energy on going from $TiCl_4$ to $TiCpCl_3$ to $TiCp_2Cl_2$, consistent with a decrease in the Cl 1s binding energy as the Ti−Cl bonds become less covalent.

The results of the ground-state DFT calculations for $TiCl_4$, $TiCpCl_3$, and $TiCp_2Cl_2$ are summarized in Tables 3 (unoccupied metal valence orbitals) and 4 (the metal 3d, 4s, and 4p character in the occupied orbitals). The optimized coordinates are provided in the Supporting Information. As shown in Table 3, $TiCl_4$ shows a significant Cl 3p contribution to all five metal 3d based orbitals, while the metal 4p orbitals contribute only to the t_2 set of d-orbitals, giving a total of 11.6% 4p character. These differences in 4p mixing can be understood in terms of group theory, as described in the analysis. In $TiCpCl_3$, the Ti d character in the five metal d-based orbitals is essentially unchanged (363% total 3d character in $TiCl_4$ vs 362% in $TiCpCl_3$); however, the metal 4p contribution has decreased significantly (from 11.6% in $TiCl_4$ to 4.4% 4p mixing in $TiCpCl_3$) and is now distributed over all five 3d orbitals. The

Table 1. Ti Pre-edge XAS Fit Results

	peak 1		peak 2				
compound	energy (eV)	intensity	energy (eV)	intensity	total intensity[a]	peak energy difference (eV)	peak intensity ratio[b]
$TiCl_4$	4969.15	58.4			58.4 ± 1.9		
$TiCpCl_3$	4968.11	22.9	4969.50	9.8	32.7 ± 2.2	1.4	2.3
$TiCp_2Cl_2$	4967.28	4.2	4968.7	5.7	9.9 ± 1.3	1.4	0.74

[a] Reported intensities are multiplied by 100. Error is based on the standard deviation of all good fits. An additional 3% error may result from normalization errors. [b] Peak intensity ratios are the ratio of the area of peak 1 divided by peak 2.

Table 2. Cl Pre-edge XAS Fit Results

compound	peak 1 energy (eV)	peak 1 int.	peak 2 energy (eV)	peak 2 int.	total int.	peak energy difference	peak int. ratio[a]	exptl % Cl 3p[b]	calcd % Cl 3p[b]
D_{2d}-$[CuCl_4]^{2-}$[c]	2820.20	0.53			0.53			7.5	
$TiCl_4$	2821.58	1.19	2822.32	1.41	2.60	0.7	0.84	37	30
$TiCpCl_3$	2821.77	1.44	2823.13	0.79	2.23	1.4	1.82	32	27
$TiCp_2Cl_2$	2821.27	0.50	2822.29	1.24	1.74	1.0	0.40	25	21

[a] Peak intensity ratios are the ratio of the area of peak 1 divided by peak 2. [b] All values given are per Ti−Cl bond. The calculated Cl 3p character comes from the DFT calculated values in Table 3. [c] Reference 42.

Table 3. Results of ADF Calculations for the Five Metal d-Based Orbitals in $TiCl_4$, $TiCpCl_3$, and $TiCp_2Cl_2$

$TiCl_4$

MO label	3E:1	3E:2	10T2:1	10T2:2	10T2:3	Total
energy (eV)	−4.886	−4.886	−4.114	−4.114	−4.114	
orb contribution:						
Ti d_{z^2}	78.68	0	0	0	0	
Ti $d_{x^2-y^2}$	0	78.68	0	0	0	
Ti d_{yz}	0	0	68.48	0	0	
Ti d_{xz}	0	0	0	68.48	0	
Ti d_{xy}	0	0	0	0	68.48	
Ti d total	78.68	78.68	68.48	69.48	68.48	362.8
Ti 4p	0	0	3.88	3.88	3.88	11.6
Cl p	20.99	20.99	23.21	23.21	23.21	111.6

$TiCpCl_3$

MO label	55A	56A	57A	58A	59A	
energy (eV)	−3.985	−3.972	−3.831	−2.603	−2.589	
orb contribution:						
Ti d_{z^2}	0.01	0.01	77.94	0.45	0.04	
Ti $d_{x^2-y^2}$	57.24	1.25	0.04	0.30	10.30	
Ti d_{yz}	1.04	10.37	0.27	53.87	6.64	
Ti d_{xz}	13.82	0.22	0.13	7.47	51.12	
Ti d_{xy}	0.80	61.01	0.07	6.29	1.07	
Ti d total	72.91	72.86	78.45	68.38	69.17	361.8
Ti 4p	0.77	0.85	1.03	0.82	0.89	4.4
Cl p	18.31	18.39	14.72	13.07	13.39	77.9
Cp total	5.85	5.76	2.91	19.01	17.88	51.4

$TiCp_2Cl_2$

MO label	64A	65A	66A	67A	68A	
energy (eV)	−3.502	−2.562	−2.437	−2.383	−2.260	
orb contribution:						
Ti d_{z^2}	3.58	2.08	0	1.94	68.09	
Ti $d_{x^2-y^2}$	68.23	0.79	0.72	0	3.14	
Ti d_{yz}	0.19	70.59	0.19	0.01	2.73	
Ti d_{xz}	0.33	0.18	4.31	67.79	1.49	
Ti d_{xy}	0.75	0.16	52.5	4.09	0.27	
Ti d total	73.08	73.80	57.72	73.83	75.72	354.2
Ti 4p	0.45	0.18	0.92	0.03	0	1.6
Cl p	15.3	2.06	16.69	1.90	6.29	42.2
Cp total	6.93	24.67	24.43	26.77	19.79	102.6

dominant Ti−Cp bonding interaction is between the e_1'' π set of Cp orbitals (in D_{5h} symmetry) and the metal d_{xz} and d_{yz} orbitals (as shown in Figure 3).[4] In $TiCp_2Cl_2$, the Ti d character has decreased only slightly (to 354% total Ti 3d character); however, the 4p mixing into the 3d set has decreased significantly to 1.6% total 4p mixing over the five 3d-orbitals. The Cp's make significant contributions to the d_{xz}, d_{yz}, d_{xy}, and d_{z^2} orbitals, while the Cl ligands interact primarily with the $d_{x^2-y^2}$ and d_{xy} orbitals. The origin of these changes will be discussed in the analysis section.

Table 4 summarizes the contributions of the metal 4s, 4p, and 3d orbitals to the filled molecular orbitals of $TiCl_4$, $TiCpCl_3$, and $TiCp_2Cl_2$. The 3d contribution to the filled MOs is essentially unchanged across this series, consistent with the similar 3d contribution to the five unoccupied metal 3d-based

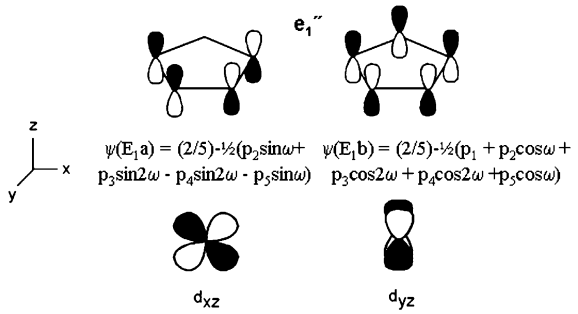

Figure 3. The e_1'' donor orbitals of Cp (top) with the LCAO-MO expressions ($\omega = 2\pi/5$) and the d-orbitals they primarily interact with (bottom).

Table 4. Comparison of Total Metal 4s, 4p, and 3d Contributions to the Filled Molecular Orbitals in $TiCl_4$, $TiCpCl_3$, and $TiCp_2Cl_2$

	4s	4p	3d
$TiCl_4$	9.6	25	114
$TiCpCl_3$	13.0	27	108
$TiCp_2Cl_2$	13.0	32	107

MOs in Table 3. The metal 4s and 4p contributions to the filled orbitals are also quite similar and if anything increase slightly in the Cp complexes. This is in apparent contrast to the decrease in 4p character in the five metal d-based orbitals, and the origin of these differences will be considered below.

IV. Analysis

A. Intensities of Ti K-Pre-edges. Quadrupole Contribution. The intensity of Ti K-pre-edge features at ~4969 eV results primarily from the mixing of metal 4p character with the metal 3d orbitals, giving this transition electric dipole allowed character. By correlating the experimentally determined intensity with the 4p character determined by DFT calculations, a linear relationship between pre-edge intensity and 4p mixing is obtained (Figure 4). Extrapolating this line to 0% 4p character gives the intensity of the pre-edge in the absence of any 4p mixing as 6.0 units or ~1.2 units of quadrupole intensity per d orbital.

Spectral Assignments and Correlations to Electronic Structure. As shown in Figure 1, the pre-edge of $TiCl_4$ has a single intense peak at ~4969 eV. This can be readily understood from group theory. In T_d symmetry, the 4p orbitals transform as t_2. The five d orbitals transform into two orbitals of e symmetry which are at lower energy (by 10 Dq of T_d) then the three d orbitals of t_2 symmetry. Hence, by symmetry the 4p orbitals will mix only with the t_2 set of d orbitals, producing a single intense peak. There will also be small quadrupole contributions to the pre-edge intensity from each of the five d orbitals. These contributions are quantitatively addressed below.

On going to $TiCpCl_3$, the symmetry of the complex is lowered and the 4p orbitals are now allowed to mix with all five 3d

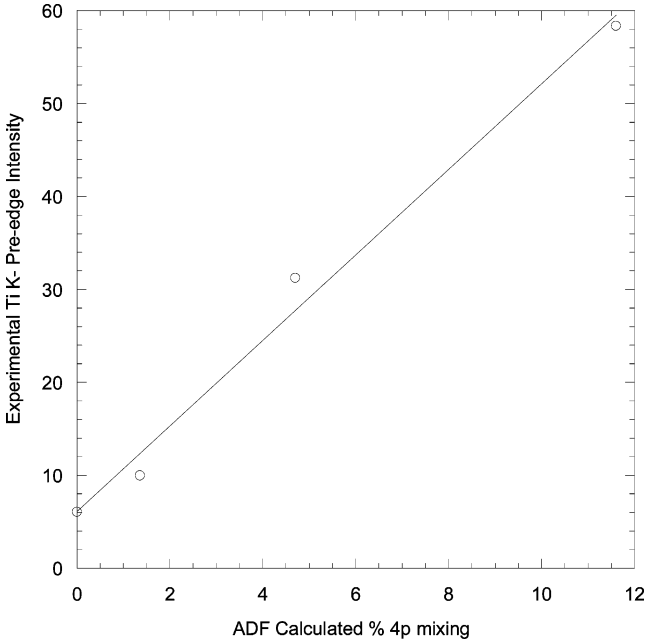

Figure 4. Total ADF calculated 4p mixing into the five 3d orbitals versus the experimental pre-edge intensity. The *y*-intercept gives the estimated quadrupole contribution to pre-edge intensity.

orbitals, which are now split in energy. The strong π donor interaction between the Cp and the metal d_{xz} and d_{yz} orbitals raises these orbitals to higher energy resulting in two peaks split by ~1.4 eV with an approximate intensity ratio of 2.3:1 in the pre-edge (Table 1). In $TiCp_2Cl_2$, the Cp ligands interact strongly with the d_{xy}, d_{xz}, d_{yz}, and d_{z^2} orbitals, raising these orbitals to higher energy and inverting the intensity distribution of the pre-edge relative to the mono-Cp complex, giving two peaks split by 1.4 eV with an intensity ratio of ~0.7:1 (Figure 1 and Table 1).

The results of ground-state DFT calculations can be correlated to the experimentally observed trends to obtain a more quantitative description of the pre-edge splittings and intensities. Using an estimated quadrupole contribution of 1.2 units per d-orbital (as determined from Figure 4 above), the remaining intensity of the $TiCl_4$ pre-edge may be assigned to the 11.6% 4p character in the t_2 set. This same intensity relationship can then be used to obtain predicted splitting and intensity ratios for $TiCpCl_3$ and $TiCp_2Cl_2$, which are compared to the experimental data in Figure 5.[40] This demonstrates that the DFT calculated ground states are good models of the electronic structures of these complexes.[41]

B. Intensities of Cl K-Pre-edges. Using D_{2d}-$Cs_2[CuCl_4]$ as a well-defined reference with 7.5% Cl 3p character per Cu−Cl bond,[42−44] the Cl 3p character per Ti−Cl bond can be determined for each of the titanium complexes. Using the experimentally determined pre-edge intensities, the Cl 3p character per Ti−Cl bond is 37%, 32%, and 25% for $TiCl_4$, $TiCpCl_3$, and $TiCp_2Cl_2$, respectively (corresponding to total Cl 3p characters of 148%, 96%, and 50% in the five d orbitals). This is consistent with the trends observed in the DFT calculations (Table 3), which also show that the addition of the Cp ligand weakens the Ti−Cl bond. However, the experimentally observed covalencies are all higher than those predicted

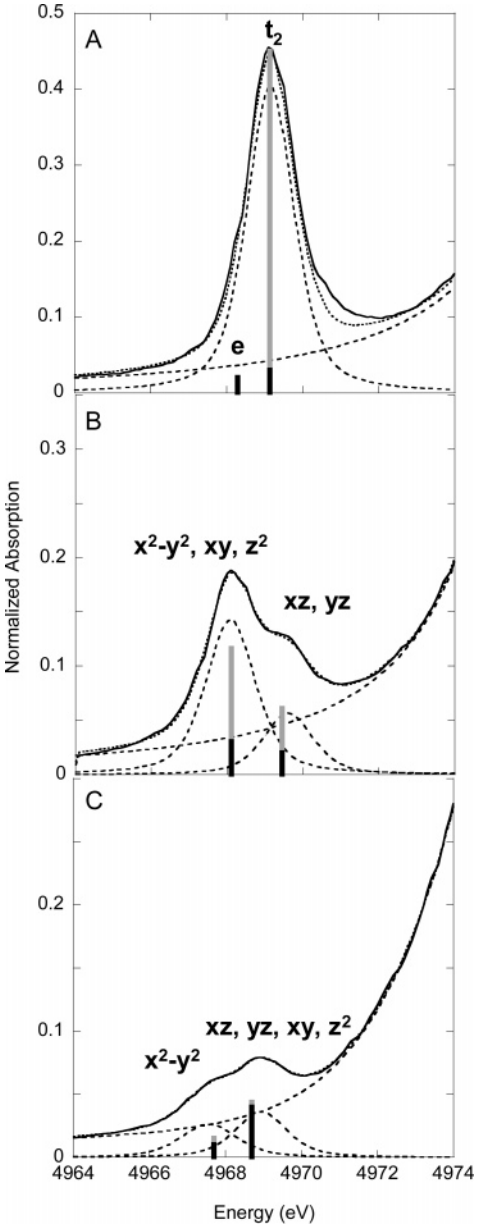

Figure 5. Ti K-pre-edge data (solid lines) and fits to data (dashed lines) for $TiCl_4$ (A), $TiCpCl_3$ (B), and $TiCp_2Cl_2$ (B). Stick plots show the energy splitting and intensity distribution predicted by DFT calculations (black bars indicate quadrupole contributions to pre-edge intensity, gray bars indicate the 4p contribution).

(40) In these complexes, dipole and quadrupole based transitions are not shifted in energy. This is in contrast to studies on infinite lattice structures were 3d−3d hybridization between neighboring Ti atoms is thought to occur. [Cabaret, D.; Joly, Y.; Renevier, H.; Natoli, C. R. *J. Synch. Rad.* **1999**, *6*, 258 and Shirley, E. L. *J. Electron Spectrosc. Relat. Phenom.* **2004**, *135*, 77.] The present study examines molecular complexes where extended lattice interactions do not complicate the bonding description.

(41) In this case, ground-state calculations were appropriate for the interpretation of the experimental splittings and intensities. This implies that the relaxation effects due to the creation of a Ti 1s core hole are relatively small. This has been verified by excited-state calculations on $TiCl_4$, which demonstrate that creation of a 1s core hole changes the d-orbital energy splittings by less than 0.2 eV and although the d-character is reduced by ×0.88, the relative intensities are essentially unchanged. A VBCI analysis which reproduces the ground-state parameters and allows for a *Q* of 4 eV for relaxation gives less than 10% intensity redistribution into shake-up satellites. Shake-up satellites are also not observed experimentally.

(42) Shadle, S. E.; Hedman, B.; Hodgson, K. O.; Solomon, E. I. *J. Am. Chem. Soc.* **1995**, *117*, 2259.

(43) Gewirth, A. A.; Cohen, S. L.; Schugar, H. J.; Solomon, E. I. *Inorg. Chem.* **1987**, *26*, 1133.

(44) Didziulis, S. V.; Cohen, S. L.; Gewirth, A. A.; Solomon, E. I. *J. Am. Chem. Soc.* **1988**, *110*, 250.

by the calculations (the DFT calculations (BP86) predict an average covalency of 30%, 27%, and 21% per Ti−Cl bond in $TiCl_4$, $TiCpCl_3$, and $TiCp_2Cl_2$, respectively). These results also parallel crystallographic trends,[37−39] which show that the length of the Ti−Cl bond increases from an average value of 2.16 Å to 2.22 Å to 2.34 Å on going from $TiCl_4$ to $TiCpCl_3$ to $TiCp_2Cl_2$, respectively.

As noted in the results, all the Cl K-edge data required at least two peaks to fit the pre-edge region. In $TiCl_4$, the two peaks correspond to the Cl 3p contributions to the e and t_2 sets of d-orbitals, hence, providing an experimental measure of differential orbital covalency. DFT calculations predict a 42% Cl 3p contribution to the e set and a 69% Cl 3p contribution to the t_2 set, split by ~0.8 eV (Table 3). Experimentally, two peaks are observed split by 0.7 eV with an approximate intensity ratio of 0.8:1 (Table 2), in reasonable agreement with the calculations. The relative ratios are difficult to accurately fit because of the overlap of the two peaks. A representative fit and its comparison to the predicted energy and intensity distributions is shown in Figure 6A.

On going to $TiCpCl_3$, the splitting of the d-orbitals has increased and the differential Cl 3p contribution to the lower and higher energy set of d-orbitals can be more clearly resolved. The fit results show a total of 62% Cl 3p character in the three lowest energy d-orbitals and 34% Cl 3p character in the two highest energy d-orbitals, giving two peaks split by 1.4 eV with an intensity ratio of ~1.8:1, in good agreement with the calculated ratio of 1.9:1 and with the energy splitting observed from the Ti K-pre-edge.[45] The highest energy d-orbitals have more significant Cp character, raising these orbitals in energy and decreasing the Cl 3p contribution. A comparison between the predicted splitting and intensity ratio and the experimental data is shown in Figure 6B.

On going to $TiCp_2Cl_2$, the d_{yz}, d_{xy}, d_{xz}, and d_{z^2} orbitals all interact strongly with the Cp decreasing the total Cl 3p character significantly and raising these four d orbitals in energy relative to the $d_{x^2-y^2}$ orbital which primarily interacts with the remaining Cl ligands. A comparison of the predicted splittings and intensity ratios with the experimental data is shown in Figure 6C.

V. Discussion

The DFT calculations are generally in very good agreement with the experimental splittings and intensity ratios of both the Ti and Cl K-pre-edge data, indicating that the calculations model the electronic structure well and may used to further aid in interpreting the spectral changes which occur on going from $TiCl_4$ to $TiCpCl_3$ to $TiCp_2Cl_2$. DFT calculations show that the total d-character in the five unoccupied d orbitals is essentially unchanged across this series; however, the 4p mixing has decreased dramatically from 11.6 to 4.4 to 1.6% for $TiCl_4$, $TiCpCl_3$, and $TiCp_2Cl_2$ respectively. In the absence of any computational results, one might interpret that the experimentally observed decrease in 4p mixing as a decrease in overall d-character is due to the replacement of Cl by a more covalent Cp ligand. However, as the calculations show, this is not the case. Although Cp is a very covalent ligand, rather than a decrease in metal d-character, the Cl covalency decreases to compensate for the presence of the Cp ligand. This is clearly observed experimentally in the Cl K-edge data, which shows a decrease in the pre-edge intensity by ~15% upon addition of each Cp resulting from a weakening of the Ti−Cl bonds.

The 4p mixing is decreasing, despite the fact that the symmetry of the site is actually lower.[46] This indicates a more complex mechanism for the observed change in 4p mixing across this series. To interpret these changes, it is important to first determine the origin of 4p mixing in $TiCl_4$.

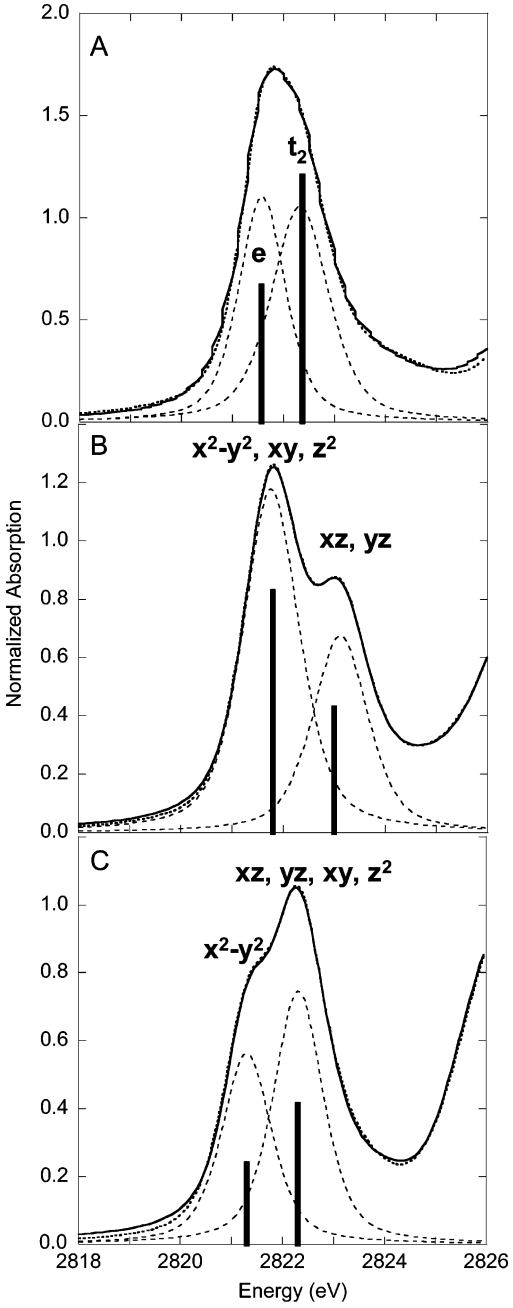

Figure 6. Cl K-pre-edge data (solid lines) and fits to data (dashed lines) for $TiCl_4$ (A), $TiCpCl_3$ (B), and $TiCp_2Cl_2$ (B). Stick plots show the energy splitting and intensity distribution predicted by DFT calculations.

(45) From Table 2, the covalency is 32% per Ti−Cl bond or a total Cl 3p covalency of 96% over the five metal 3d orbitals. Using the relative intensity ratios of the two pre-edge peaks (Table 2), it is determined that 62% Cl 3p character will be in the three lowest energy d-orbitals and 34% will be in the two highest energy d-orbitals.

(46) Calculations on hypothetical $TiCl_4$ structures of C_{3v} and C_{2v} symmetry (in which one C_{3v} or two C_{2v} of the Ti−Cl bonds was fixed 0.1 Å longer and the remaining coordinates were allowed to geometry optimize with symmetry constraints) predict a slight increase (~1%) in 4p mixing relative to T_d $TiCl_4$.

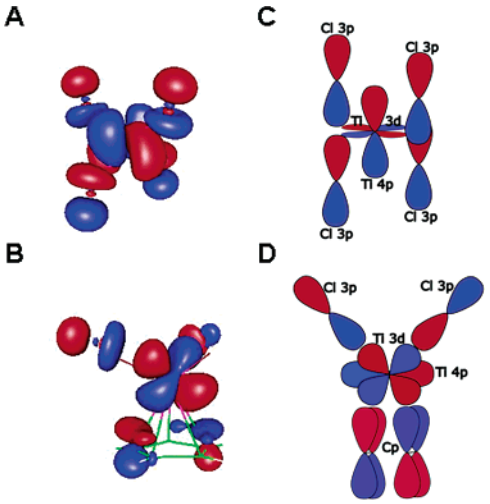

Figure 7. Contour plots for MO 10T2:3 of $TiCl_4$ (A) and MO 58A of $TiCpCl_3$ (B). Schematics showing the proposed mechanism for metal 3d−4p mixing via ligand overlap in $TiCl_4$ (d_{xy} with p_z) (C) and the "phase effect" between the ligand and metal 4p orbitals in $TiCpCl_3$ (d_{yz} with p_y) (D).

Ligand-Based Origin of the 4p Contribution to Pre-edge Intensity: The Ti−Cl Bond. As described above, the Ti K-pre-edge intensity in $TiCl_4$ results from mixing of the metal 4p orbitals with the metal 3d orbitals of t_2 symmetry. This group theory allowed mixing can be visualized by examining the molecular orbitals of $TiCl_4$. The t_2 set of d orbitals all have Cl ligand orbitals that have the appropriate symmetry to overlap with both the metal 3d and metal 4p orbitals. Figure 7 shows the contour of one of the t_2 orbitals of $TiCl_4$ (Figure 7A) and a schematic including the metal 4p orbitals (shown to larger scale to aid in visualization, Figure 7C). Here, the metal $3d_{xy}$ and $4p_z$ both mix via sigma bonding interactions with the Cl 3p orbitals. This mechanism can be described using a configuration interaction (CI) model.[47,48] The 3 × 3 matrix shown below accounts for the interaction of the ligand p orbitals with the metal 3d and the metal 4p orbitals.

	$\|Cl3p\rangle$	$\|Ti3d\rangle$	$\|Ti4p\rangle$
$\langle Cl3p\|$	0	T_1	T_2
$\langle Ti3d\|$	T_1	Δ_1	0
$\langle Ti4p\|$	T_2	0	Δ_2

The Cl ligand based orbital configuration is at lowest energy. The metal 3d and metal 4p configurations are at higher energy, with the energy separations corresponding to Δ_1 and Δ_2. T_1 is the interaction matrix element between the ligand p and metal d orbitals and T_2 is the interaction matrix element between the ligand p and metal 4p orbitals. In this model, there is no matrix element allowing for direct interaction of the metal 3d and metal 4p orbitals. (This is likely the physical basis for the angular overlap model in references 49−51, which invokes a direct matrix element between the metal 3d and 4s orbitals to allow for 3d−4s mixing.) Diagonalization of this matrix gives the ground-state eigenvectors. By choosing reasonable values of T's and Δ's, the ground-state energy splittings and wave function coefficients can be reasonably reproduced.[52] This model provides a ligand based configuration interaction mechanism for metal 3d−4p mixing and quantitates the involvement of the 4p orbitals in ligand−metal bonding. Thus, in $TiCl_4$, the experimental pre-edge intensity provides a direct experimental measure of the metal 3d−4p mixing and an indirect measure of Ti 4p-Cl bonding.

Nature of the Ti−Cp Bond and Contributions to 4p Mixing. For $TiCpCl_3$ and $TiCp_2Cl_2$, the metal 4p contribution to bonding is more complex. The pre-edge intensities clearly show that the 4p contribution to the 3d orbitals has decreased upon replacement of a Cl ligand by Cp. There are several possible explanations for this. First, the Cp is very covalent and has a strong π-type donor interaction with the titanium d-orbitals (the d_{xz} and d_{yz} orbitals in $TiCpCl_3$), which decreases the bonding interaction of the titanium with the Cl ligands. If the only mechanism for 3d−4p mixing is via the overlap with the Cl ligands, then one might expect as the Ti−Cl overlap decreases the 4p mixing would also decrease. The decrease in Ti−Cl covalency is one factor that contributes to the decrease in pre-edge intensity. This explanation though does not allow for the Cp ligand orbitals to mix with metal 4p orbitals and would require that the 4p contribution to bonding decreased. However, the metal 4p contribution to the filled orbitals is very similar and in fact is slightly increased in both $TiCpCl_3$ and $TiCp_2Cl_2$ relative to $TiCl_4$ (Table 4), indicating that the metal 4p (and 4s) orbitals contribute to Cp−Ti bonding. This suggests that there is an additional effect impacting the Cl induced 3d−4p mixing.

Examination of the calculated metal d based orbitals provides insight into a possible mechanism for the decreased 3d−4p mixing in the Cp complexes. Figure 7 gives the contour of the primarily d_{yz} based molecular orbital of $TiCpCl_3$ (MO 58A, Figure 7B and Table 3) and a schematic of this orbital with contributions from the Cl and Cp ligand orbitals and from the metal 4p orbitals. (The 4p orbitals are shown at a larger scale to aid in visualization.) When the Cl 3p orbitals have a bonding relationship with the metal 4p orbital, the Cp ligand orbital will necessarily have an antibonding relationship with the metal 4p orbital. This "phase effect" is a result of the symmetry of the d_{xz} and d_{yz} orbitals, which both have significant Cp and Cl ligand contributions which are antibonding and dictate the phase relationship of the Cp and the chloride ligands. This results in a net interference effect between the ligand overlap contributions to 4p mixing resulting in a decreased 3d−4p contribution to the d orbitals.

This effect can also be evaluated computationally. Fixed point calculations on hypothetical $TiCpCl_3$ structures show that when the Cp ligand is moved 0.3 Å away from the Ti (while keeping the Ti−Cl distances fixed), the 4p contribution to the five 3 d-orbitals increases by ∼1% (despite a decrease in the 4p contribution to the filled orbitals). Conversely, when the Ti−Cp distance is decreased the 4p mixing into the 3d orbitals decreases further (while the 4p contribution to the filled orbitals increases). A similar phase effect also accounts for the decreased intensity in $TiCp_2Cl_2$.

(47) van der Laan, G.; Westra, C.; Haas, C.; Sawatzky, G. A. *Phys. Rev. B* **1981**, *23*, 4369.
(48) Davis, L. C. *Phys. Rev. B* **1982**, *25*, 2912.
(49) Smith, D. W. *Inorg. Cim. Acta* **1977**, *22*, 107.
(50) Schäffer, C. E. *Inorg. Chim. Acta* **1995**, *240*, 581.
(51) Hitchman, M. A.; Cassidy, P. J. *Inorg. Chem.* **1979**, *18*, 1745.

(52) Using $\Delta_1 = 4$ eV, $\Delta_2 = 10$ eV, $T_1 = 3.5$ eV, and $T_2 = 2.0$ eV gives a metal d-based ground state with 75% 3d character, 20% Cl 3p character, and 5% 4p mixing.

This phase effect can be modeled by extending the configuration interaction model to include inequivalent ligands. The 4×4 matrix is given below.

	$\|Cp\rangle$	$\|Cl3p\rangle$	$\|Ti3d\rangle$	$\|Ti4p\rangle$
$\langle Cp\|$	0	0	T_1	T_2
$\langle Cl3p\|$	0	Δ_1	T_3	T_4
$\langle Ti3d\|$	T_1	T_3	Δ_2	0
$\langle Ti4p\|$	T_2	T_4	0	Δ_3

The Cp based ligand orbital configuration is lowest in energy, with the Cl based ligand orbital, the metal 3d orbital, and the metal 4p orbital configurations at higher energy by Δ_1, Δ_2, and Δ_3, respectively. T_1 is the interaction matrix element between the Cp ligand and the metal d orbitals and T_2 is the interaction matrix element between the Cp ligand and metal 4p orbitals. T_3 and T_4 define the Cl−Ti 3d and Cl−Ti 4p interactions, respectively. As in the 3×3 model, there is no matrix element allowing for direct interaction of the metal 3d and metal 4p orbitals. There is also no matrix element allowing for direct Cp and Cl ligand interaction. In this model, if the Cp−Ti 4p (T_2) and Cl−Ti 4p (T_4) interaction matrix elements have the same sign, there is significant 4p mixing into the 3d orbitals. However, if T_2 and T_4 are opposite in sign (as in Figure 7B, D), the 4p mixing into the 3d orbitals decreases, providing a CI demonstration for the phase effect in reducing pre-edge intensity.

Summary. The results of this study demonstrate that Cp is a strong donor which decreases the interaction of the titanium with the remaining "spectator" ligands, resulting in longer, less covalent Ti−Cl bonds. This may have important implications for the labilization of chloride in $TiCp_2Cl_2$ and may also provide some insight into the reduced antitumor activity of $TiCpCl_3$.[11]

Using $TiCl_4$ as a reference, the mechanism of 3d−4p mixing has been established using a configuration interaction model which demonstrates that ligand overlap (i.e., covalent bonding) with both the metal 3d and metal 4p orbitals allows for the metal 3d and 4p orbitals to mix. This is directly measured in the pre-edge and indicates that pre-edge intensities may be used to define ligand−metal covalency in molecular Ti(IV) complexes in noncentrosymmetric environments. Further, as demonstrated by the $TiCpCl_3$ and $TiCp_2Cl_2$ complexes, this correlation may have interference effects from strong bonding interactions with different ligand types.

Acknowledgment. We thank Prof. Robert Waymouth and Dr. Kuo-Wei Huang for providing $TiCl_4$, $TiCpCl_3$, and $TiCp_2Cl_2$. SSRL operations are funded by the Department of Energy, Office of Basic Energy Sciences. The Structural Molecular Biology program is supported by the National Institutes of Health, National Center for Research Resources, Biomedical Technology Program and by the Department of Energy, Office of Biological and Environmental Research.

Supporting Information Available: Geometry optimized Cartesian coordinates of $TiCl_4$, $TiCpCl_3$, and $TiCp_2Cl_2$. This material is available free of charge via the Internet at http://pubs.acs.org.

JA044827V